

# STATISTICAL IDENTIFICATION AND OPTIMAL CONTROL OF THERMAL POWER PLANTS

H. NAKAMURA AND Y. TOYOTA

*Kyushu Denki-Seizo Company, Technical Department, 19-18, Shimizu 4-chome, Minami-ku,  
Fukuoka 815, Japan*

(Received October 15, 1987; Revised February 5, 1988)

**Abstract.** Statistical system identification and its use for the optimal control of thermal power plants are discussed. The analysis of the plant dynamics and derivation of the state-space representation are performed by fitting a multivariate AR model to the plant data obtained by an experiment. The basic concept of the power plant control and the motivation that necessitated the statistical approach are explained in the introduction. Practical procedure for the implementation of the method is described in detail with examples obtained from actual plants. The main items discussed are the selection of system variables by means of relative power contribution analysis, determination of the state equation and adjustment of the optimal feedback gain by digital simulation technique. Finally, excellent performance of the proposed control system is demonstrated by the operating records of 500 MW and 600 MW supercritical plants.

*Key words and phrases:* Statistical method, AR model, system identification, thermal power plant, supercritical boiler, multivariable system, nonlinear system, steam temperature control, digital simulation.

## 1. Introduction

In a large capacity high-pressure high-temperature boiler for electric power generation, deviations from the set points of steam temperatures at the boiler outlet must be kept within one or two percent of their rated values in order to maintain the nominal operating efficiency and ensure the safety and the maximum equipment life of the plant. The main purpose of the boiler control is to allow the increase or decrease of steam generation as fast as possible in response to the load command from the power system's dispatch center, while satisfying the above-mentioned operating conditions.

However, since a modern thermal power plant usually includes many control loops with significant mutual interactions within the boiler process, it is not easy for the conventional PID controller to fully compensate for these

interactions and satisfy the required steam conditions for large and fast changes of plant load. This difficulty of controlling a mutually interacting multivariable system had been one of the principal factors that set the limit to the response of a thermal power plant to the load changes required for the load-frequency control (LFC) of an electric power system.

More than twenty years ago, the first named author of this paper started an investigation for improving load following capability of thermal power plants. In the study, which was carried out under the collaboration with Kyushu University, several block diagrams representing boiler dynamics were obtained through a series of theoretical and experimental works. Based on these diagrams boiler simulation models for the study of controller tuning were composed with a large-scale analog computer, and later with a digital computer. However, in spite of the laborious investigation on these simulation models, no decisive conclusion was found on how to improve the control performance of the integrated system.

This was due to the fact that parameters in the conventional PID controller had different influences on different controlled variables. This experience led the author to realize the difficulty of tuning a multivariable system, i.e., a multi-input and multi-output (MIMO) system, and consequently to distrust the "optimal tuning" of conventional PID controllers in MIMO systems.

The author then learned the theory of optimal control. Impressed deeply by its prominent design concept, he tried to apply the theory to the boiler control. However, the trial which continued for a couple of years finally failed, because of the difficulty of deriving a state space representation of the complex boiler process. This showed that, so long as we stuck to the conventional approach based on the simultaneous differential equations representing the energy and mass balances in the process, the derivation of the state equation for practical use would be almost impossible.

In the mean time, Otomo *et al.* (1972) reported a successful implementation of the optimal control system for a cement kiln process, where the method of statistical system analysis and controller design had been adopted. This led the author to the investigation of the optimal control of power plants by means of the statistical approach. Experimental studies were repeated using a digital computer, an analog-digital hybrid computer, and also an exact power plant model established on a power plant simulator in the Central Research Institute of Electric Power Industries of Japan. Finally an optimal control system to be called ADC (Advanced Digital Control, Nakamura and Akaike (1981)) was established. The first optimal control system was implemented in February 1978 at Buzen No. 1 plant, a 500 MW supercritical plant of Kyushu Electric Power Company. As anticipated in the stage of simulation studies, the improvement of the control performance realized by the optimal regulator was quite remarkable. As of 1987, five supercritical plants with the total capacity of 2,700 MW are in commercial operation in Kyushu Electric Power

Company. With their high load following capability, these plants are significantly contributing to the load-frequency control, LFC, of the company's power system.

In this paper, we first give an outline of the thermal power plant control so as to provide the readers with the general idea of the difficulties and problems underlying the actual plant control.

Practical aspects of the statistical system identification and controller design are explained with examples obtained from actual plants and simulation models. Finally, the effectiveness of the optimal control system based on the statistical approach is demonstrated with the results of field test and routine operation of the actual plants. Technical aspects of the analysis and controller design are summarized in Appendix.

## 2. Control of a power plant

In this section, we will discuss the control of a power plant equipped with a supercritical once-through boiler. For convenience sake we provide the list of abbreviated notations of various variables in Table 1.

When the change in load command (MWC) takes place, boiler input variables are manipulated through feedforward and feedback control loops. Of these control loops, the feedforward loops work to adjust the input

Table 1. Nomenclature.

FR	Fuel flow rate
GD	Opening of the reheater flue gas damper in the rear path of the boiler shell
MW	Generator output power
MWC	Megawatt command or load command issued from the system's dispatch center to the plant
MWD	Megawatt or load demand measured at the load changing rate setter outlet
RHT	Reheater outlet steam temperature (Deviation from the set-point value)
SHT	Superheater outlet steam temperature (Deviation from the set-point value)
SP	Flow rate of the superheater spray water
TP	Main steam pressure (Deviation from the set-point value)
WWT	Waterwall outlet fluid temperature (Transient deviation from the exponentially smoothed mean value)

variables, such as the governing valve opening, the flue gas damper opening (GD), fuel flow rate (FR), feedwater flow rate, etc., to the values corresponding to the new required load (MW). Since the manipulation of each input variable has influence on more than one output variables in different manners, controlled variables, such as main steam pressure (TP), superheater outlet steam temperature (SHT), reheater outlet steam temperature (RHT), etc., deviate from their set-points.

To cancel such deviations, feedback loops connecting controlled variables with manipulated variables adjust boiler inputs so as to achieve final thermal-hydraulic balance in the boiler process. However, as these feedback control loops interact with each other within the boiler process, they form a typical mutually interacting multivariable system. This has been the principal factor that limited load changing rate of the thermal power plants and led to the introduction of the "Advanced Digital Control" system to be described in this paper.

In the case of a supercritical variable-pressure boiler, which has been widely adopted recently, the above-mentioned situation becomes more serious, because in a variable-pressure boiler, its main steam pressure is controlled to vary in proportion to the boiler load. This causes changes of the temperature of working fluid within the evaporator tubes which is approximately at the saturation temperature of the pressure and enhances the nonlinearity of the process. The above fact also means that for the load change of a variable-pressure boiler a larger amount of feedforward fuel control is necessary to complement the energy variation within the boiler.

From the above discussion, it can be said that the key to the boiler control is to find optimal coordination of the feedforward and feedback loops and good compensation for the interactions within the boiler process.

### 3. Fundamental requirements for the implementation of optimal control system

The design of an optimal control system, or an optimal regulator, is performed based on the state equation, which is a state space representation of the system in the time domain. In this sense, the state equation is the only means that relates the actual system to the controller design. Thus, the basic problem in the implementation of an optimal regulator is how to obtain practically useful state equation.

Here, by the term "practically useful" the authors mean the following fundamental requirements that the state equation should be endowed with.

(1) The state equation must describe the system dynamics with a required accuracy; needless to say, this is a prerequisite for realizing a satisfactory performance of the control system.

(2) The state equation must be a reduced order mathematical model which is compact enough to be handled by a process control computer; this

requirement comes from the aspect of on-line control, because our process control computer usually deals with many tasks on a time-sharing base, and although the highest priority is given to the computation for the on-line control, the state equation and state-feedback gain matrices with relatively small sizes are desirable from the viewpoint of lessening the computer load.

(3) Derivation of the state equation and the controller design must be easy and simple enough to be carried out by a well-talented plant engineer rather than a specialist with expertise on the analysis of the process dynamics and modern control theory; this is important to make the adoption of the new sophisticated system as a common practice in the future.

(4) The optimal regulator designed on the basis of the state equation must be robust enough; i.e., it must maintain the expected performance against possible changes in the process dynamics due to the fouling and slugging of boiler tubes or the change of the fuel mixing rate, etc.

As a method satisfying the above requirements the statistical system identification and controller design procedure originally developed by Akaike (1971) and successfully applied to the cement kiln control (Otomo *et al.* (1972)) was adopted for the present power plant control.

#### 4. Optimal control system

The control system is realized in the form

$$Z(n) = FZ(n - 1) + Gu(n - 1) + W(n) ,$$

$$x(n) = HZ(n) ,$$

$$u(n) = KZ(n) ,$$

where  $Z(n)$  denotes the state of the system,  $u(n)$  the control input to the manipulated variables,  $W(n)$  a white noise and  $x(n)$  the system output or the controlled variables. The controller gain  $K$  is designed so as to minimize a performance criterion

$$J_I = E \sum_{n=1}^I [Z'(n)QZ(n) + u'(n - 1)Ru(n - 1)] .$$

Procedures for the analysis and identification of the power plant system characteristics and for the design of an optimal controller are described in Appendix.

Figure 1 shows the configuration of the ADC (Advanced Digital Control) system proposed by the authors. As shown in the figure, the plant, consisting of the boiler-turbine process and the conventional PID controller, is regarded as the object system of the computer control. Variables such as steam temperatures along the boiler tube, and other necessary process

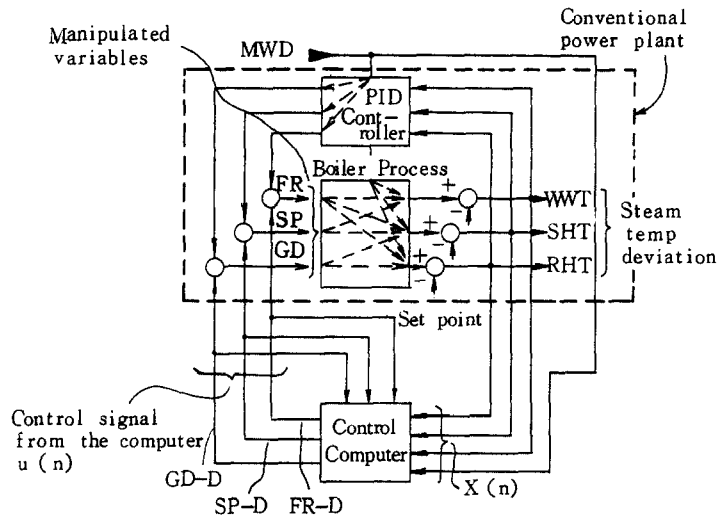


Fig. 1. Conceptual diagram of ADC system.

variables define the output  $x(n)$  and are taken into the computer. The vector  $u(n)$  of control signals to the manipulated variables, such as the fuel flow rate, spray flow rate, RH flue gas damper opening, is computed, together with the state variable  $Z(n)$ , by the algorithm prepared in the computer and added via the D/A converters to the control signals from the PID controller at the summing amplifiers at every control period. It should be noted that the exogenous variable MWD is included as a "controlled" variable.

## 5. Procedure for the design of ADC system

In this section we will discuss details of the procedure for the design of the optimal regulator ADC of thermal power plants by using examples taken from actual plants.

### 5.1 Preliminary experiment

#### *Selection of system variables*

Selection of proper system variables is important to obtain a suitable state equation. It should be avoided to include in the model more than one state variables that show similar responses to the change of a certain manipulated variable, because such variables can cause an ill-conditioned property of the coefficient matrices of the AR model. In the selection of the system variables, the knowledge of the process is indispensable. The relative power contribution analysis to be described under the heading MULNOS is also helpful for this purpose.

*Rough estimate of plant dynamics*

Prior to the implementation of the ADC system it is desirable to make a rough estimate of the response of the controlled variables to the stepwise change in each of the manipulated variables and MWD. Such step response curves are converted into frequency response function curves to determine the approximate frequency ranges of the test signals to be employed in the system identification experiment.

Figure 2 shows an example of the amplitude gains of the frequency response function curves (MWD to SHT and MWD to RHT) which were obtained in this manner in a 600 MW supercritical variable-pressure plant.

5.2 *Data acquisition for system identification*

*Statistical properties of the test signals*

The vector time series data for AR-model fitting are obtained in the system identification experiment. As the test signal to stimulate the system a pseudo-random binary time series (maximum period sequence or *m*-sequence) produced in the computer is used for each manipulated variable and MWD after being modified by a two-stage digital low-pass filter.

The amplitude and the fundamental period of the *m*-sequence and the parameters of the digital low-pass filter are determined for each test signal to cover the required frequency range which is roughly estimated from the frequency response function curves obtained from the preliminary experiment.

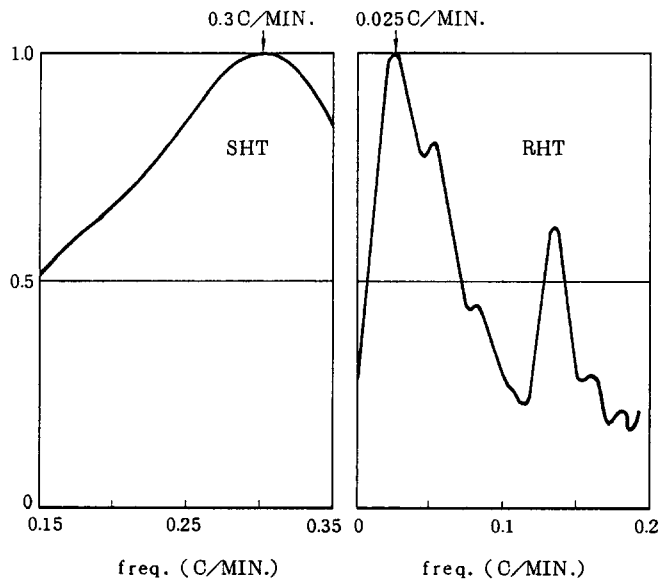


Fig. 2. Frequency response function of SHT and RHT obtained by conversion from step response function.

Figure 3 is an example of the power spectra of SHT, RHT and test signals computed from the record of the system identification experiment of a 600 MW plant. In this experiment a filter consisting of two cascaded first-order-lag digital filters was used with the exponential smoothing factor  $\alpha$ . The sampling period was 30 seconds. The unit period of  $m$ -sequence  $\Delta$  and the smoothing coefficients of the digital filter  $\alpha$  were chosen to the values indicated in Fig. 3 so that the power of the test signals was concentrated in the frequency ranges where the power spectra of SHT and RHT were significant.

#### Data acquisition

In the system identification experiment, test signals produced in the computer are simultaneously applied to the actuators of the MWD and other manipulated variables via D/A converters. The data of the system variables are recorded in the computer for several hours at every equi-spaced time interval,  $\Delta t$ . Figure 4 shows a portion of the record obtained at a 600 MW plant. The sampling period  $\Delta t$  and the data length differ depending upon the dynamics of the plant. Generally speaking, sampling period of 20 to 40 seconds and data length of 5 to 8 hours give satisfactory results. Usually, system identification experiments are performed at two or three load levels for the purpose of nonlinearity compensation, which will be explained in the later section.

### 5.3 System analysis and controller design

The off-line computation programs for system analysis and controller design are stored in the plant computer. They consist of programs taken from the package TIMSAC (Akaike and Nakagawa (1972)) and some of their modifications. The functions of these programs are described below: for

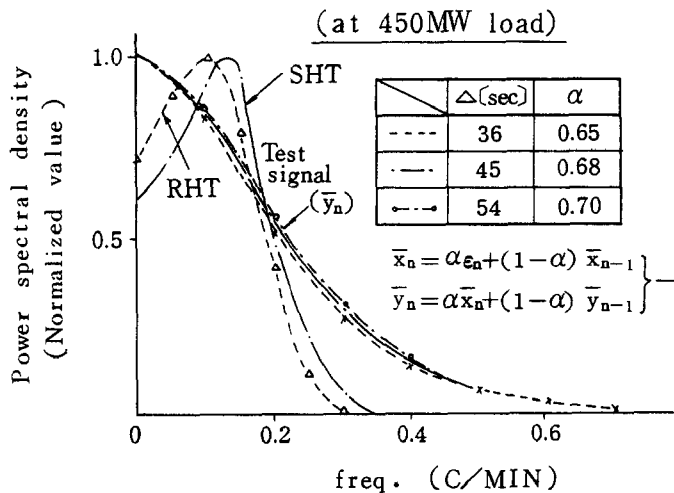


Fig. 3. Power spectra of controlled variables and test signals.



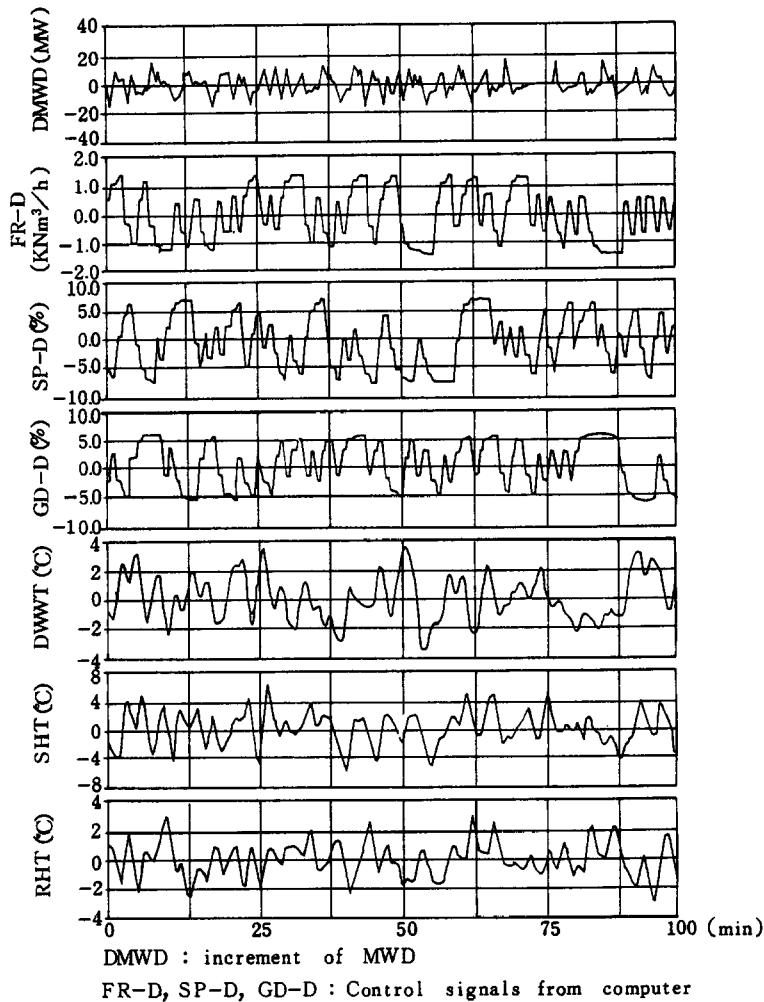


Fig. 4. Records of system identification experiment.

further details readers are referred to the book by Akaike and Nakagawa (1972).

**MULCOR:** This program calculates the covariance matrices of the system variables from the data obtained in the system identification experiment.

**MFPE:** Using the covariance matrices, this program computes the coefficient matrices of the multi-variate AR model by solving the Yule-Walker equation by Levinson-Whittle type fast algorithm. The model order is automatically determined by a criterion function MFPE.

**MULRSP:** Rational spectral density functions of the multivariable system are computed by equation (A.5) in Appendix.

**MULNOS:** Assuming the orthogonality between the elements of the innovation vector  $W(n)$  in equation (A.2) in Appendix, MULNOS computes contribution of the elements of  $W(n)$  to the system variables. Figure 5 shows an example of the relative power contribution (solid lines) of  $W(n)$  to the variance of WWT, SHT and RHT, which were obtained at three different loads of a 600 MW plant. In the figure, power spectral density function of

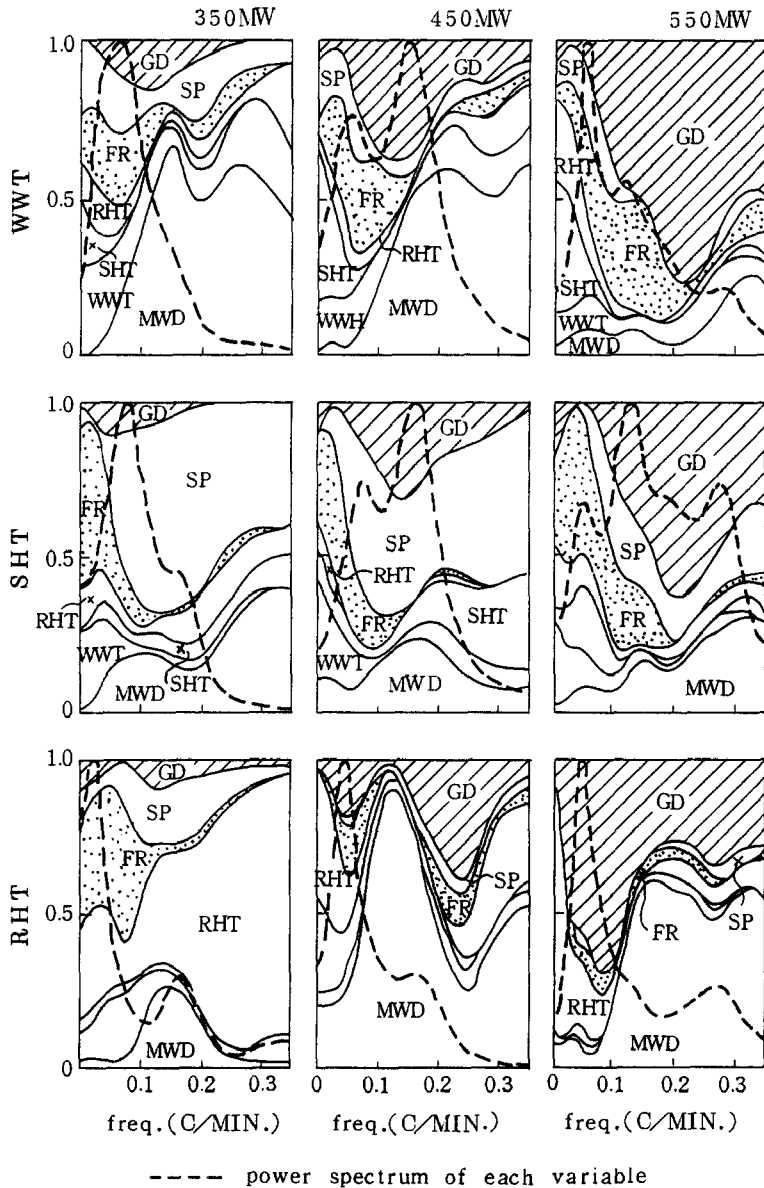


Fig. 5. Relative power contribution of a 600 MW supercritical plant.

WWT, SHT and RHT are also shown in dotted lines.

The figure tells that in the variation of WWT and SHT at 550 MW and 450 MW, contributions from FR are dominant in the low frequency range below 0.1 cycle/min, while in the frequency range above 0.05 or 0.1 cycle/min contributions of SP, GD, to SHT are significant. It is also observed that GD and MWD have significant contributions to the variance of RHT.

As for the differences between the different loads, relatively significant contribution from GD to RHT at the load 550 MW reduces at the plant load decreases, and at 350 MW, GD has minor contribution to the process variables compared with MWD and other manipulated variables. This fact indicates that in the low load region, where the opening of the flue gas damper is large, the manipulation of GD has only small control capability. Such observation is quite helpful in determining proper controller gain for each manipulated variable in accordance with load levels.

*FPEC:* By this program, the state equation is derived through AR model fitting in the way described in Section A.3 in Appendix. As the result of the computation the elements of the state transition matrix  $F$  and the manipulation matrix  $G$  in equation (A.11) are obtained. Here a criterion FPEC is used for the model order determination in place of MFPE in AR model fitting.

*OPTDES:* In accordance with the procedure described in Section A.4, this program computes the optimal state-feedback gain matrix using Dynamic Programming (D.P.) under the quadratic criterion function. As the result of the D.P. computation the gain matrix  $K_I$  in equation (A.13) is obtained.

*DIGITAL SIMULATION:* By this program, validity of the state equation and appropriateness of the state-feedback gain matrix are checked by digital simulation as follows:

*Checking the state equation:* By comparing the responses of the actual plant with the simulation results obtained by using the state equation, the validity of the state equation can be verified. Figure 6 shows a comparison between the plant dynamics and the results of digital simulations which were obtained for a 500 MW plant. In this checking the actual record of the system identification experiment is compared with the record of digital simulation, in which the signals of MWD, FR, SP, GD having the same magnitudes and patterns as those of the actual plant record were used in the state equation.

*Estimation of control performance:* The above-mentioned digital simulation is also used for the adjustment of the state-feedback gain matrix. In this case, in addition to the MWD changes the control signals computed from  $u(n) = K_I Z(n)$  are provided to the state equation at each step of the state transition. The weighting matrices  $Q$  and  $R$  are adjusted by observing both the behavior of the state variables and the amplitudes of the manipulated variables.

In the optimal controller design procedure, D.P. computation and digital simulation are repeatedly performed with revised  $Q$  and  $R$  at each iteration

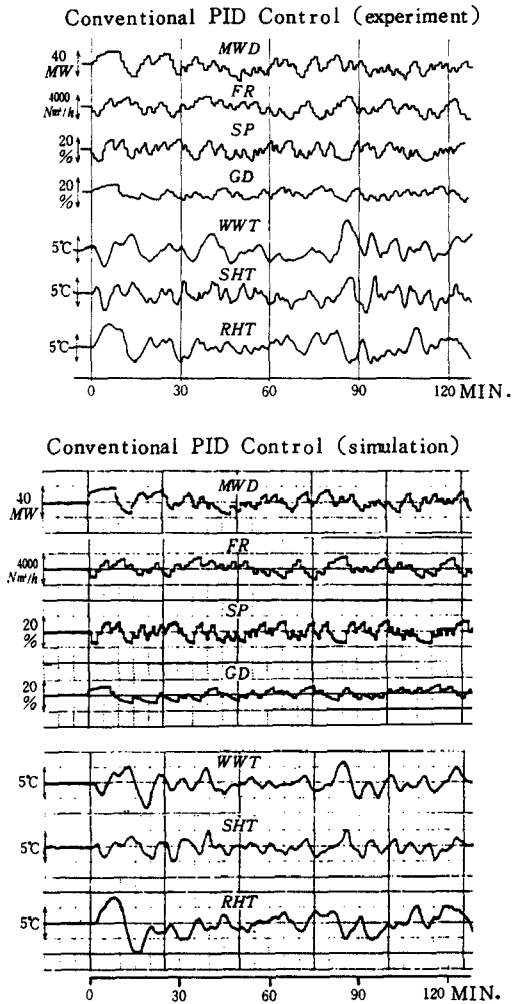


Fig. 6. Comparison of the plant data and digital simulation results.

step, until several candidates of the gain matrix for the field test are finally obtained.

An example of this kind of simulation study is shown in Fig. 7. As can be seen in the figure the fluctuations of WWT, SHT and RHT operating under the same MWD changes are remarkably reduced by the ADC optimal control compared with those by the conventional PID controller. It is also observed that the amplitudes of FR, SP, GD, the control signals from the computer, are well within allowable ranges.

*Compensation for plant nonlinearity:* In order to compensate for the significant output-power dependence of the characteristics of the boiler process, system identification is performed at two or three load levels. In the

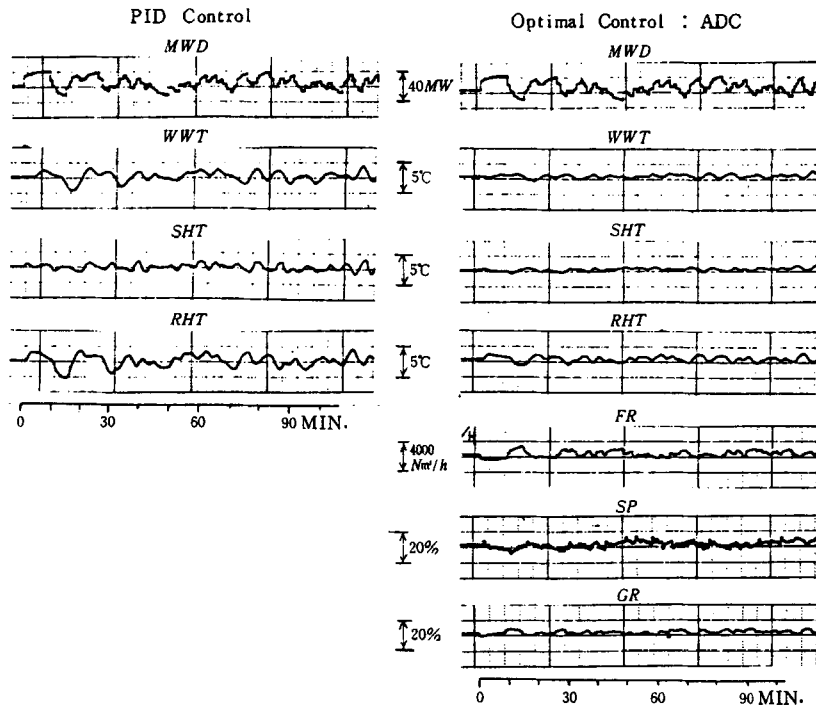


Fig. 7. Preliminary adjustment of optimal feedback gain by means of digital simulation.

actual operation, the parameters in the state equation and the state-feedback gain matrix are adjusted at each control time by taking linear interpolation of these identified models with weights determined by the magnitude of MWD.

Experiments using an elaborate power plant model of Central Research Institute of Electric Power Industries of Japan revealed that for a large rampwise load change the load-adaptive adjustment of control parameters considerably reduces the amplitudes of the responses of both steam temperatures and manipulated variables compared with the results obtained by the system with parameters fixed (Nakamura and Akaike (1981)).

The validity of the parameter adjustment can be checked by digital simulation. Figure 8 shows a comparison of actual 500 MW plant records and digital simulation results under a large amount of rampwise load changes at the rate of 25 MW per minute. As shown in the figure the results of the simulation show practically sufficient agreement to the records of the actual plant.

*Importance of including MWD in the state-variable vector:* In our system MWD, the largest disturbance to the plant, is included in the state-variable vector as illustrated in Fig. 9. MWD is effective for the prediction of the behavior of SHT and RHT, and consequently for a better control of these variables.

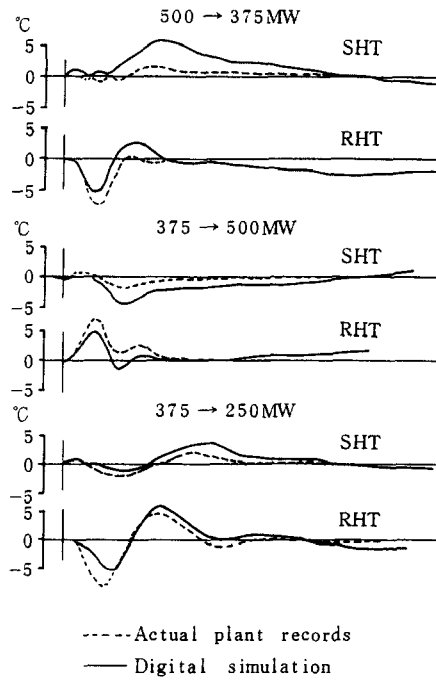


Fig. 8. Results verifying the effectiveness of the load-adaptive parameter adjustment.

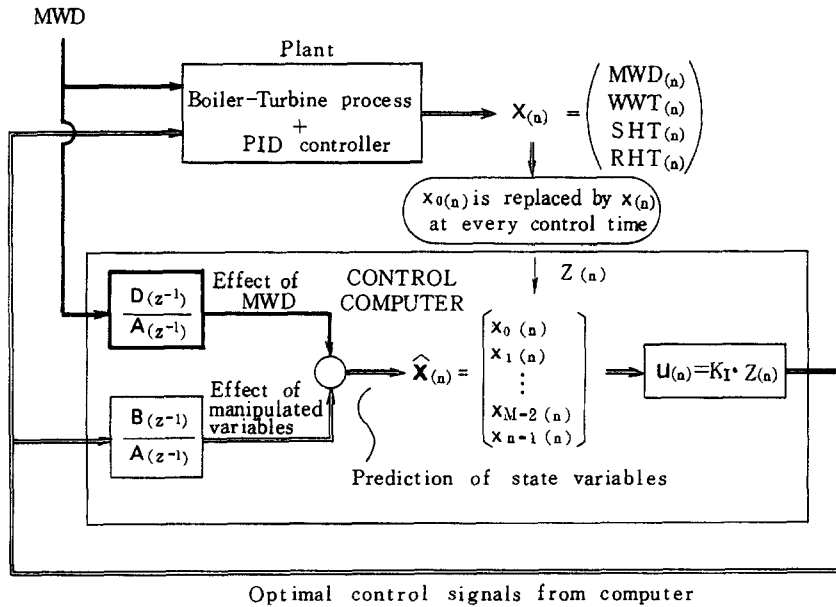


Fig. 9. Block diagram explaining the effectiveness of including MWD as a pseudo state variable.

The importance of including MWD signal in the state-variable vector is also confirmed by an experiment. Figure 10 is a result obtained with a large-scale simulation model of a 500 MW variable-pressure plant which was used in the preliminary study for the implementation of the optimal regulator. In the figure, are shown response curves of steam temperatures and control signals from the computer against a 25 MW stepwise load change. In Fig. 10, (a) is the case when seven system variables, MWD, WWT, SHT, RHT, FR, SP, GD, are used, while (b) is the case when six system variables are used with MWD excluded. Symbols with suffix FF such as FR-FF, indicate feed-

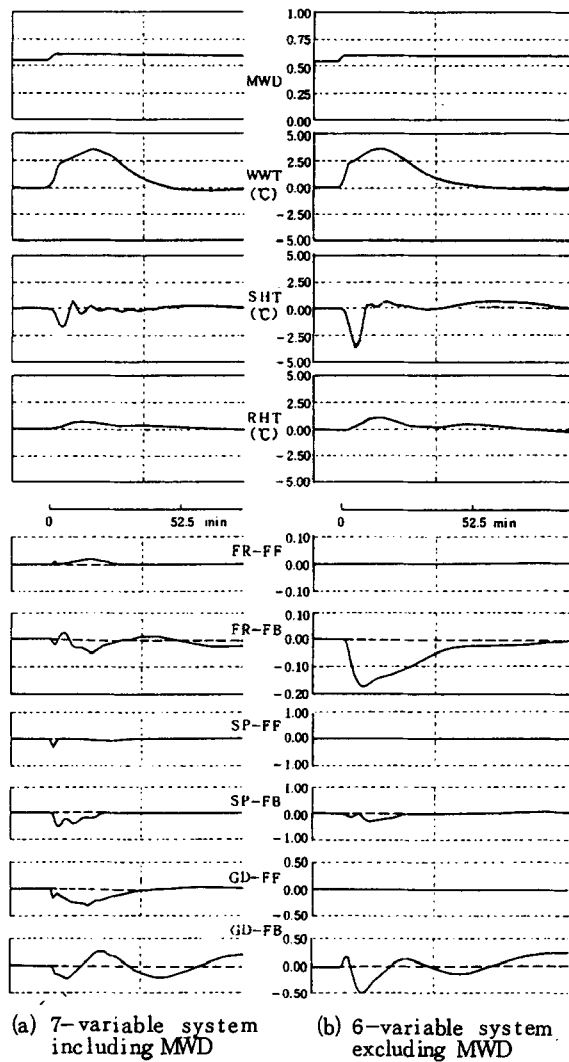


Fig. 10. Experimental results demonstrating the effectiveness of including MWD in the state vector.

forward signals determined by the MWD change, and symbols with suffix FB such as FR-FB, denote feedback signals composed from the deviations of WWT, SHT and RHT.

It is clearly seen that in the seven-variable system the feedforward signals determined on the basis of prediction act quite timely to reduce not only the steam-temperature deviations, but also the amplitudes of the control signals.

*Further consideration on the elements of the state-variable vector:* The importance of including MWD in the state-variable vector can be evaluated from the relative power contribution analysis. Figure 11 is an example, in which the relative power contributions of system variables to SHT and RHT are analysed.

It is observed that the hatched portions, which express the power

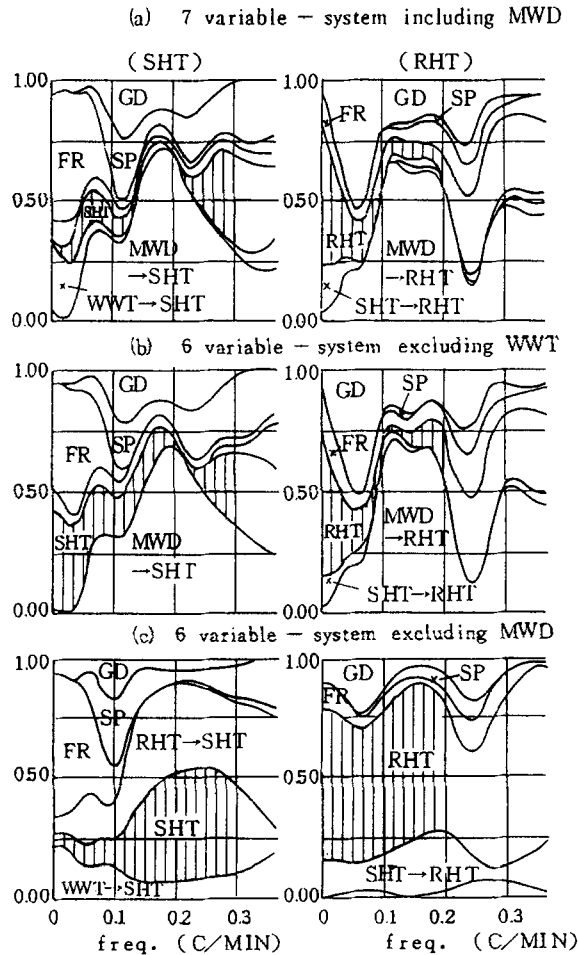


Fig. 11. Selection of system variables by means of relative power contribution analysis.



inherent to the variation of SHT or RHT themselves i.e., the power not relevant to other system variables, are quite large for the model (c) with MWD excluded, especially in RHT. It is also seen in (b) that the contribution from WWT to SHT is relatively large in the low frequency range.

From the above observation the seven system variables including MWD and WWT are used in the final model building.

#### 5.4 *Adjustment of the weighting matrix $Q$ and $R$*

The most elaborate part in the optimal controller design is the proper choice of the coefficients in the weighting matrices  $Q$  and  $R$  in equation (A.13). The following is an approach to this problem:

(1) The coefficient corresponding to MWD in  $Q$  is put to zero to permit the free movement of MWD, because MWD is non-manipulable.

(2) The state-feedback gain matrix is obtained by the D.P. computation with proper initial choice of the elements in  $Q$  and  $R$ , which can be easily revised by observing the results of the following steps, (3) and (4).

(3) Digital simulation of the optimal control using specified random input of MWD is performed and the behavior of the system variables is recorded.

(4) From the record of the simulation data, compute the power spectra of the controlled variables and the variances of the manipulated variables are computed and evaluated. In our plant computer the time required for the computation of steps (2) through (4) is less than 10 minutes.

Power spectra of the controlled variables SHT and RHT, and variances of the manipulated variables FR, SP, GD, corresponding to several choices of the weighting matrices  $Q$ ,  $R$ , allow us to estimate the influence of the elements of  $Q$  and  $R$ . By combining this observation with that of relative power contributions of FR, SP, GD to SHT and RHT, we can find proper choice of  $Q$  and  $R$ . For further fine adjustment of  $Q$  and  $R$ , the method suggested by Nakamura and Uchida (1984) is also helpful, in which the elements of  $Q$  and  $R$  that provide specified variances of manipulated variables under an assumed MWD variations are obtained automatically by the iteration procedure through (2) to (4) described above.

## 6. Field test results

The ADC system can be applied to both the constant-pressure and variable-pressure boilers. As a rule, finer tuning of the PID controller is required in variable-pressure boilers than in constant-pressure boilers to compensate for the system non-linearities. Results obtained with actual plants will be presented in this section.

### 6.1 *600 MW supercritical constant-pressure plant*

Figure 12 shows a comparison of the behavior of the manipulated

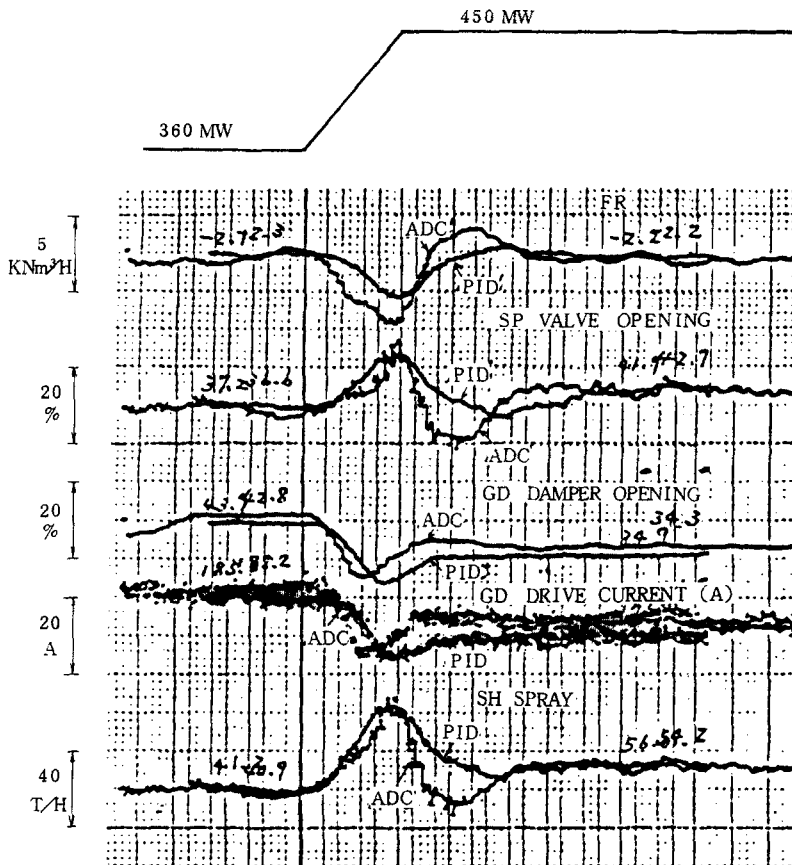


Fig. 12. Comparison of the response of the identical rampwise load change.

variables in the ADC system and that in the PID controller under the identical rampwise change in MWD shown at the top of the figure of a 600 MW plant. As can be seen manipulated variables FR, SP, GD, respond more quickly to the MWD change in the ADC system than in the PID controller. Cross correlation functions between MWD and the manipulated variables for each system under stationary operating conditions are shown in Fig. 13. The time differences between the zero axis and the peak points of the cross correlation curves show approximately the delays of the manipulated variables to the MWD changes.

By observing these figures, it may be said that the manipulated variables respond faster in the ADC system than in the PID controller. This quicker response of the manipulated variables in the ADC system is apparently realized by the use of the predicted state variables for the control signal synthesis.

Similar analysis with a power plant simulator showed faster response of

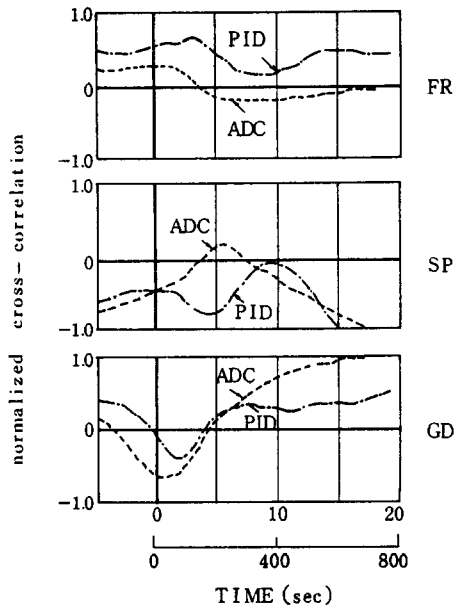


Fig. 13. Comparison of the correlation functions between MWD and manipulated variables.

the seven-variable ADC system with MWD in the state-variable than the six-variable ADC system without MWD. This result also verified the appropriateness of including MWD in the state vector.

In Fig. 14 the control performance of the ADC system in routine operation is compared with that of the conventional PID controller under similar operating conditions. Considerable improvement of SHT and RHT control can be seen by the figure.

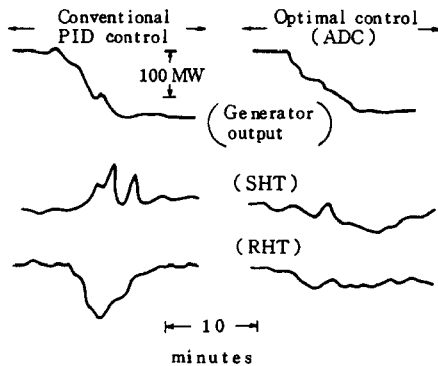


Fig. 14. Comparison of control performance during routine operation.

In general it is said that in the well-tuned optimal control not only the fluctuations of the controlled variables SHT and RHT, but the amplitudes of manipulated variables such as FR, SP, GD are smaller than those of the PID control.

## 6.2 500 MW supercritical plants

Figures 15 and 16 show the records obtained in the routine operation of two supercritical constant-pressure plants. In the figures the plant control was respectively switched from ADC to PID control and from PID to ADC in the midst of the record to demonstrate the excellent control performance of the ADC system. In Fig. 16 feedforward control signals computed by applying Linear Programming procedure developed by Uchida *et al.* (1981) were added to those of the original ADC system.

The ADC system was also applied to a 500 MW supercritical variable-pressure plant, which is a typical process with strong non-linearity and mutual interactions within the boiler (Uchida *et al.* (1986)). Although some difficulties were experienced in the case of the variable-pressure plant, it was concluded that, if deliberately planned preliminary studies were carried out on a plant simulator in advance, the improvement of the control performance produced by the introduction of ADC system is considerable even for this case. Figure 17 is a comparison of the records obtained under the ADC and PID control systems in the field test of the variable-pressure plant. The reduction of deviations are particularly significant with RHT.

## 7. Conclusion

The optimal control system ADC discussed in this paper has been in routine operation since 1978. Since its first implementation at a 500 MW supercritical plant, the ADC system has practically experienced no trouble. Operating experiences during these nine years have revealed outstanding features of the system as described below.

By the adoption of the ADC system, the behavior of the plant becomes quite calm even under the LFC (Load-Frequency Control) operation of the power system where the plant is often subjected to large, quick, frequent load changes. This result suggests that the ADC controllers have sufficient stabilities to allow their performances under severe operating conditions. Such performance is realized by the LQ (Linear Quadratic) controller which quickly brings the deviations of the process variables back to their specified values by properly eliminating mutual interferences between the process variables.

The implementation of the ADC system is usually performed at the final stage of the plant construction. By our experience, in spite of the gradual change in process dynamics due to the seasoning effect of the boiler, the deterioration of the actuators, etc., no plant has ever necessitated readjust-

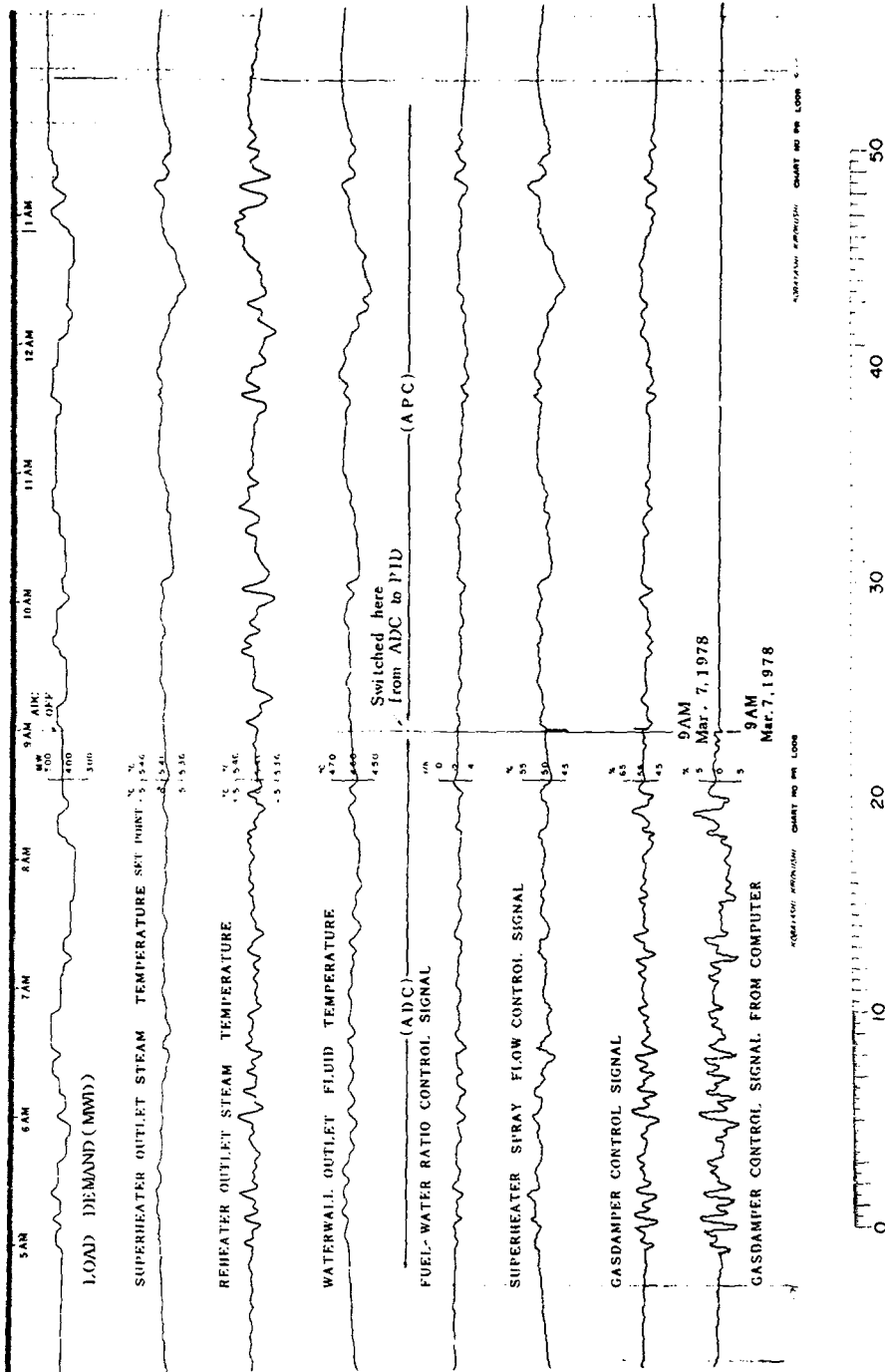


Fig. 15. Control performance of the ADC system and PID control system (500 MW supercritical constant pressure plant, Buzen No. 1).

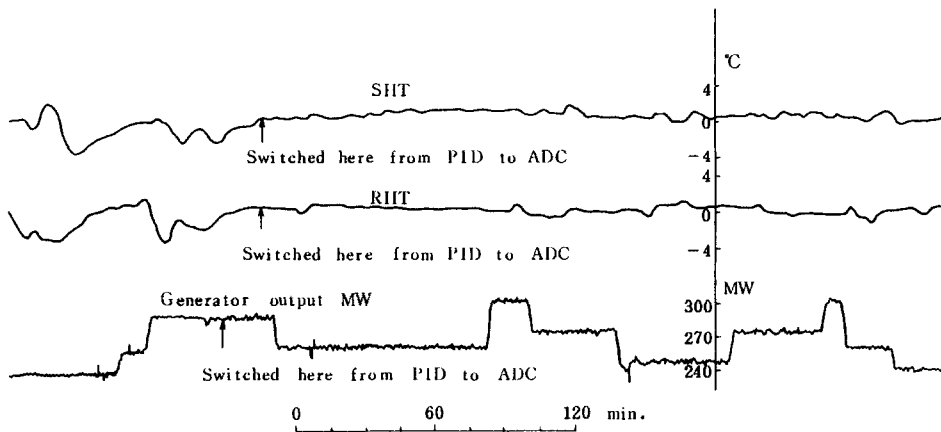


Fig. 16. Control performance of the ADC system and PID control system (500 MW supercritical constant pressure plant, Buzen No. 2).

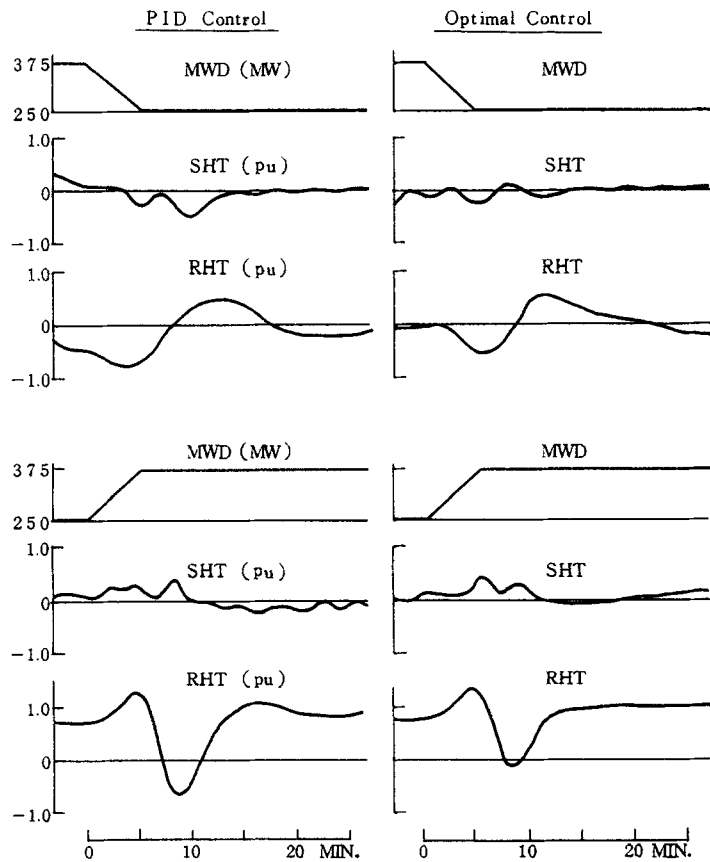


Fig. 17. Control performance of the ADC system and PID control system (500 MW supercritical variable pressure plant).

ment of the control parameters since its inauguration. This fact clearly demonstrates the robustness of the ADC system.

Another feature of the ADC system that should be emphasized is the simplicity of the design and maintenances. Since all the programs required for the system identification and controller design are stored in the plant computer, even a plant engineer with some knowledge of the system can easily perform the design and maintenance work with the help of the instruction manual. This is an important aspect for a technique to survive for generations.

### Acknowledgements

The authors would like to express their appreciation to Professor H. Akaike of the Institute of Statistical Mathematics, Mr. M. Uchida of the Kyushu Electric Power Company for their continuous cooperation and to Dr. H. Mizutani and Dr. T. Kitami of the Central Research Institute of Electric Power Industries of Japan for their collaborations in the investigation and implementation of the ADC system. Thanks are also due to the members of Kyushu Electric Power Company, Toshiba Corporation, Mitsubishi Electric Corporation, Ishikawajima-Harima Heavy Industries Co., Ltd., Mitsubishi Heavy Industries, Ltd., Kyokuto Boeki Kaisha, Ltd. and Bailey Japan Co., Ltd. who participated in the implementation of ADC systems.

### Appendix

For the convenience of readers, we provide here a brief review of the theory and method developed in a series of papers by Akaike (1968, 1971) for the statistical analysis and identification of a system and the optimal regulator design. The book by Akaike and Nakagawa (1972) discusses the method in detail with the cement kiln process as an example of its application. Akaike (1978) also provides a convenient introduction.

Consider a time series of  $k$ -dimensional vector  $X(n)$ , consisting of the data sampled at every time interval of  $\Delta t$  (henceforth referred to as the system variable vector), whose elements are the variables describing the behavior of the system. Now, we denote by  $u(n)$  an  $l$ -dimensional subvector consisting of manipulated variables, and by  $x(n)$  an  $r$ -dimensional subvector composed of the rest of the components of  $X(n)$ . Then, we get

$$(A.1) \quad X(n) = \begin{bmatrix} x(n) \\ u(n) \end{bmatrix} \begin{matrix} \uparrow r \\ \uparrow l \end{matrix} \begin{matrix} \uparrow k \\ \downarrow \end{matrix} .$$

The vector  $x(n)$  is composed of the variables expressing process dynamics and

non-controllable “exogenous” variables which will be useful for predicting the behavior of the system.

### A.1. Expression of the system by AR model

First, we fit an AR (autoregressive) model to  $X(n)$  in the following way:

- (1) Subtract from the system variables’ data their mean values to produce a data series  $X(n)$ ,  $n=1, 2, \dots, N$ .
- (2) Compute sample auto- and cross-covariance matrices of  $X(n)$ .
- (3) Fit an AR model to  $X(n)$ ,  $n=1, 2, \dots, N$  to obtain

$$(A.2) \quad X(n) = \sum_{m=1}^M A(m)X(n-m) + W(n),$$

where  $A(m)$ ,  $m=1, 2, \dots, M$  are the coefficient matrices,  $M$  is the order of the model, and  $W(n)$ , the innovation, is a vector white noise. The  $A(m)$ ’s that minimize variances of the components of  $W(n)$  are obtained by solving a multivariate Yule-Waker equation.

- (4) The model order  $M$  is determined through the minimum AIC procedure, where the AIC is defined by

$$(A.3) \quad \text{AIC} = (-2)\log(\text{maximum likelihood}) \\ + 2 (\text{number of free parameters}).$$

The minimum AIC procedure selects the model with the minimum value of AIC from a set of models defined with the parameters determined by the method of maximum likelihood. Under the Gaussian assumption the criterion FPE (Final Prediction Error) which was formerly introduced by Akaike (1971) for the order determination of an AR model satisfies the asymptotic equality

$$(A.4) \quad \text{AIC} = N \log \text{FPE}.$$

In our analysis, particular types of FPE, the MFPE and FPEC, were used for model order determination; see TIMSAC in Akaike and Nakagawa (1972).

### A.2. System analysis by means of relative power contribution

Once the AR model expression is obtained in the form of equation (A.2), we can reproduce a time series which is statistically equivalent to the original time series  $X(n)$  by using the coefficient matrices  $A(m)$ ,  $m=1, 2, \dots, M$ . Here, the innovation vector  $W(n)$ , a white Gaussian noise vector with variances of specified values, is used as the input signal to produce the autoregressive process. The relative power contribution analysis to be described below is



introduced based on this concept.

From the autoregressive model equation (A.2) we can get the following relationship

$$(A.5) \quad P(f) = (A(f))^{-1} S (A(f))^*{}^{-1},$$

where  $P(f)$  denotes the spectral density matrix,  $S$  denotes the innovation variance matrix  $E[W(n)W(n)']$ ,

$$A(f) = I - \sum_{m=1}^M A(m) \exp(-i2\pi fm)$$

and  $*$  denotes conjugate transpose. The  $(i, j)$  element of  $P(f)$  and  $S$  will be denoted by  $P_{ij}(f)$  and  $\delta_{ij}$ , respectively. Assuming the orthogonality between the components of  $W(n)$ , we get  $S = \text{diag}(\delta_{11}, \delta_{22}, \dots, \delta_{kk})$ , which denotes the diagonal matrix with its  $i$ -th diagonal element  $\delta_{ii}$ . With this assumption we get the decomposition

$$(A.6) \quad P_{ii}(f) = \sum_{j=1}^k b_{ji}(f)^2 \delta_{jj},$$

where  $b_{ij}(f)$  denotes the  $(i, j)$  element of  $A(f)^{-1}$ . The relative power contribution of  $w_j(n)$  to  $x_i(n)$  is defined by

$$(A.7) \quad r_{ij}(f) = \frac{b_{ij}(f)^2 \delta_{jj}}{P_{ii}(f)}.$$

The cumulative relative power contribution from  $w_1(n), w_2(n), \dots, w_j(n)$  to  $x_i(n)$  is defined by

$$(A.8) \quad R_{ij}(f) = \sum_{h=1}^j r_{jh}(f) \quad j = 1, 2, \dots, k.$$

The vertical distance between the graphs  $[R_{ij}(f); 0 \leq f \leq 1/2\Delta t]$  and  $[R_{i,j-1}(f); 0 \leq f \leq 1/2\Delta t]$  shows the relative power contribution  $r_{ij}(f)$ .

### A.3. State space representation of the system dynamics

From the multivariate AR model expressed by equation (A.2) we get

$$(A.9) \quad x(n) = \sum_{m=1}^M a_m x(n-m) + \sum_{m=1}^M b_m u(n-m) + w(n),$$

where  $w(n)$  is the vector composed of the first  $r$  components of  $w(n)$  and  $a_m$

and  $b_m$  are defined by the relation

$$A(m) = \begin{array}{c} \left. \begin{array}{c} \leftarrow r \rightarrow \leftarrow l \rightarrow \\ \left[ \begin{array}{cc} a_m & b_m \\ * & * \end{array} \right] \\ \downarrow l \end{array} \right\} \end{array}.$$

If we define  $r$ -dimensional vectors  $x_0(n), x_1(n), \dots, x_{M-1}(n)$  by

$$\begin{aligned} x_0(n) &= x(n) \\ x_k(n) &= \sum_{m=k+1}^M [a_m x(n+k-m) + b_m u(n+k-m)] \\ & \qquad \qquad \qquad k = 1, 2, \dots, M-1, \end{aligned}$$

then we get

$$\begin{aligned} (A.10) \quad & x_0(n) = a_1 x_0(n-1) + b_1 u(n-1) + x_1(n-1) + w(n), \\ & x_1(n) = a_2 x_0(n-1) + b_2 u(n-1) + x_2(n-1), \\ & \quad \vdots \qquad \qquad \qquad \quad \vdots \\ & x_{M-1}(n) = a_M x_0(n-1) + b_M u(n-1), \end{aligned}$$

which will be expressed in the matrix form as

$$\begin{aligned} (A.11) \quad & Z(n) = FZ(n-1) + Gu(n-1) + W(n), \\ & x(n) = HZ(n), \end{aligned}$$

where

$$\begin{aligned} Z(n) &= \begin{bmatrix} x_0(n) \\ x_1(n) \\ \vdots \\ x_{M-2}(n) \\ x_{M-1}(n) \end{bmatrix}, & F &= \begin{bmatrix} a_1 & I & 0 & \cdots & 0 \\ a_2 & 0 & I & \cdots & 0 \\ \vdots & \vdots & & & \\ a_{M-1} & 0 & 0 & \cdots & I \\ a_M & 0 & 0 & \cdots & 0 \end{bmatrix}, \\ G &= \begin{bmatrix} b_1 \\ b_2 \\ \vdots \\ b_{M-1} \\ b_M \end{bmatrix}, & W(n) &= \begin{bmatrix} w(n) \\ 0 \\ \vdots \\ 0 \\ 0 \end{bmatrix}, \\ H &= [I \ 0 \ \cdots \ 0]. \end{aligned}$$

Equation (A.11) is the state space representation or the state equation, which is commonly called ‘‘observable canonical form’’, or ‘‘observable companion form’’.

#### A.4. Design of LQ (Linear Quadratic) optimal regulator

For the system given in the previous section

$$(A.12) \quad \begin{aligned} Z(n) &= FZ(n-1) + Gu(n-1) + W(n), \\ x(n) &= HZ(n), \end{aligned}$$

the optimal control system under a quadratic criterion function, or the Linear Quadratic optimal regulator, is realized by choosing such  $u(n)$ 's which minimize

$$(A.13) \quad J_I = E \sum_{n=1}^I [Z'(n)QZ(n) + u'(n-1)Ru(n-1)],$$

where  $I$  is a properly chosen integer and the matrix  $Q$  is non-negative definite and  $R$  is positive definite and  $'$  denotes transpose.

We have

$$J_I = E[Z'(I)QZ(I) + u'(I-1)Ru(I-1)] + J_{I-1},$$

where, from (A.12), we have

$$\begin{aligned} E[Z'(I)QZ(I)] &= E[FZ(I-1) + Gu(I-1)]' \\ &\quad \cdot Q[FZ(I-1) + Gu(I-1)] \\ &\quad + EW'(I)QW(I). \end{aligned}$$

Thus  $u(I-1)$  that minimized  $J_I$  must minimize  $[Z'(I-1)F' + u'(I-1)G']Q[FZ(I-1) + Gu(I-1)] + u'(I-1)Ru(I-1)$  and is given by

$$u(I-1) = -(R + G'QG)^{-1}G'QFZ(I-1).$$

Proceeding successively to the next stage we get the following computation scheme:

$$\begin{aligned} P_0 &= Q \\ M_i &= P_{i-1} - P_{i-1}G(R + G'P_{i-1}G)^{-1}G'P_{i-1} \\ P_i &= F'M_iF + Q \end{aligned} \quad i = 1, 2, \dots, I-1,$$

and

$$\begin{aligned} u(I-i) &= K_iZ(I-i) \\ K_i &= -(R + G'P_{i-1}G)^{-1}G'P_{i-1}F \quad i = 1, 2, \dots, I. \end{aligned}$$

To realize a stationary control we increase  $I$  until  $K_I$  stabilizes and put

$$(A.14) \quad u(n) = K_I Z(n) .$$

This defines our feedback control. A proper choice of the matrices  $Q$  and  $R$  can be made with the aid of the digital simulation experiments as described in the text.

#### REFERENCES

- Akaike, H. (1968). On the use of a linear model for the identification of feedback systems, *Ann. Inst. Statist. Math.*, **21**, 243–247.
- Akaike, H. (1971). Autoregressive model fitting for control, *Ann. Inst. Statist. Math.*, **23**, 163–180.
- Akaike, H. (1976). Canonical correlation analysis of time series and the use of an information criterion, *System Identification: Advances and Case Studies*, (eds. R. H. Mehra and D. G. Lainiotis), 27–96, Academic Press, New York.
- Akaike, H. (1978). On the identification of state space models and their use in control, *Direction in Time Series*, (eds. D. R. Brillinger and G. C. Tiao), 175–187, The Institute of Mathematical Statistics, Hayward, California.
- Akaike, H. and Nakagawa, T. (1972). *Statistical Analysis and Control of Dynamic Systems*, Saiensu-sha, Tokyo (in Japanese, with a computer program package TIMSAC written in FORTRAN IV with English comments. English version of the book is to be published by Kluwer Scientific Publishers).
- Nakamura, H. and Akaike, H. (1981). Statistical identification for optimal control of supercritical thermal power plants, *Automatica—J. IFAC*, **17**, 143–155.
- Nakamura, H. and Uchida, M. (1984). Practical procedure for optimal regulator implementation of thermal power plants, *9th IFAC world congress, Control of power stations and systems, Session 01.1/D*.
- Otomo, T., Nakagawa, T. and Akaike, H. (1972). Statistical approach to computer control of cement rotary kilns, *Automatica—J. IFAC*, **8**, 35.
- Uchida, M., Nakamura, H. and Kawai, K. (1981). Application of linear programming to thermal power plant control, *8th IFAC world congress, Kyoto*, 97-2.
- Uchida, M., Nakamura, H., Toyota, Y. and Kushihashi, M. (1986). Implementation of optimal control at a supercritical variable-pressure thermal power plant, *Proc. IFAC Symposium, Beijing, People's Republic of China*.